WIENER-BASED INTERFEROMETRIC SIGNATURE RECONSTRUCTION

Marc HONIKEL
Federal Institute of Technology, Zurich, Switzerland
Institute for Geodesy and Photogrammetry
marc.honikel@geod.baug.ethz.ch

Working Group II

KEY WORDS: Interferometry, DEM, Simulation, Reconstruction, Data Fusion

ABSTRACT

After almost ten years of regular spaceborne SAR data supply, various microwave remote sensing techniques are established today. Among them, SAR interferometry (InSAR) and its applications like digital elevation model (DEM) generation or surface change detection may be the most exciting ones, which the recent shuttle radar topography mission (SRTM) has proved impressively. SAR interferometry takes advantage from the phase signal properties and is used to derive the topographic height of an image pixel. The interferometric phase (i.e. the phase difference between two sensor positions and the target) is a measure for the travel path length difference of the SAR waves proportional to the target height. Nevertheless, some SAR system inherent limitations corrupt these measurements and leave areas inaccessible for the interferometric examination, limiting the use of interferometry especially in steep terrain. This paper addresses the reconstruction of the interferometric signature with a new approach based on the Wiener signal restoration principle, which distinguishes between more and less noise affected interferometric phase values, thus considering the partially extreme signal-to-noise (SNR) differences within an interferogram. The interferometric phase is estimated with help of a synthetic interferogram derived from a stereo-optical DEM, which serves as a complementary data source. In this way, an estimate of the phase is retrieved even in regions of low signal to noise ratio, which in turn improves the quality of the InSAR DEM measurement.
The procedure is applied to an interferogram derived from an ERS-1 image pair and a photogrammetric DEM from SPOT data. All treated phase degradations have been removed enabling precise DEM generation. The resulting DEM surpassed by far the initial stereo-optical and InSAR DEMs in completeness and accuracy, thus proving the power of the proposed technique.

1 INTRODUCTION

By mapping about 80% of the landmass of the world interferometrically, the successful shuttle radar topography mission will help spreading InSAR DEM data into mid-scale databases. In order to derive the height of a point from the interferometric phase measurements, the phase ambiguities, coming from the 2π measurement interval, must first be solved with the so-called phase unwrapping, adding the correct multiple of 2π to each phase value. Phase unwrapping becomes extremely difficult in cases of low SNR, due to signal decorrelation. Although single-pass phase measurements do not suffer from temporal decorrelation of the phases, which restricts massively the use of InSAR height measurements from spaceborne repeat-pass systems, the system inherent measurement limitations remain. InSAR height measurements are restricted to terrain not steeper than the viewing angle of the sensor, leaving mountainous regions inaccessible for interferometric analysis. In addition to the terrain inclination, the signal interaction with certain types of vegetation, causing multiple scattering or phase jumps, affect the measurements locally and act as an additional local noise source.

InSAR height information may serve for the enhancement of existing DEM databases, up to now consisting mainly of photogrammetrically derived DEMs. Through its generation process, point matching and following interpolation, stereo-optical DEM quality is less terrain dependent than its SAR counterpart. On the other hand, stereo-optical DEM generation also suffers from system limitations like cloud occlusions or texture dependency of the matching process, resulting in measurement holes.
Because of the different data and generation principles, the height measurements of both DEM sources can be assumed to be uncorrelated. Therefore, when introduced the generation process of their counterpart, the data will enhance the information content of a scene. The following sections deal with the possibility of overcoming the InSAR limitations by fusing InSAR with a stereo-optical DEM data, which are used complementarily to the SAR measurements.
The complementarity of both optical and SAR height measurements has already been used for different fusion approaches for the improvement of DEMs from remote sensing data (Honikel, 1998, 1999). In one case, optical height

measurements served as an approximation of the mean terrain shape, while details from the interferometric DEM were added. In the other case, weights have been introduced to the fusion process, which indicated the local height error. In both cases, the height error decreased significantly after the fusion.
The Wiener-based method, which is proposed in this paper, unifies these approaches, for the processing of interferometric phase measurements. The data are fused by taking advantage from having a general approximation from an independent data source and knowledge of the expected error of each measurement. With the great deal of information available through the introduction of the simulated interferogram, the filter is realized by modeling the ideal phase course and then fitting the model to the observation. It is intended to improve the interferometric height determination process by restoration of the noise-corrupted interferometric phase measurements, thus easing the noise-sensitive phase unwrapping process and taking full advantage of the InSAR height accuracy, which is theoretically limited by the SAR wavelength (cm-scale!).

2 WIENER PHASE ESTIMATION

The reduction of the phase noise is crucial for the correct determination of the multiple 2π, which has to be added to each phase value during the unwrapping process. In presence of noise, phase jumps (residuals) can occur, which spoil the implicit unwrapping assumption of a smooth terrain, with phase changes not higher than π between two adjacent values. The unwrapping is bound to fail, if these measurements are not excluded from the procedure. Common automated phase unwrapping techniques, e.g. using ghost-lines (Goldstein, 1988), are able to deal with this problem only to a certain extent. Large regions of low SNR still lead either to failure of the DEM generation process, or, worse, add a global error also to uncorrupted phase measurements, if unwrapped erroneously. Zebker (1994) gives an evaluation of InSAR errors and topographic map accuracy for ERS-1.
Common approaches of noise reduction include multi-look image processing, averaging or interferogram filtering. All these techniques have in common that they are hardly noise adaptive, thus affecting also valid measurements while dealing with the noise. The phase reconstruction in regions, where the interferometric measurement fails (e.g. due to layover) is generally not possible with these methods. The proposed method aims therefore at a restoration process, which not only removes or reduces the noise, but also restores these regions, where the phase measurement previously failed.

2.1 Interferometric phase restoration model

The following considerations relate to the general degradation and restoration model, given in Fig. 1, in which the image vector f is subject to some unspecified type of degradation, which affects the image both spatially (multiplicatively), resulting in a blurred image g_b, and pointwise (additively), resulting in an observation g.
Applied to the interferometric phase, degradation causes both, a local blurring of the fringe lines and adds to the local noise. Especially blurring of the fringe lines endangers correct phase unwrapping, as the border between the phase cycles is not determinable, resulting possibly in coarse unwrapping errors. Fig. 6 and 8 illustrate these effects, occurring due to layover and temporal decorrelation.

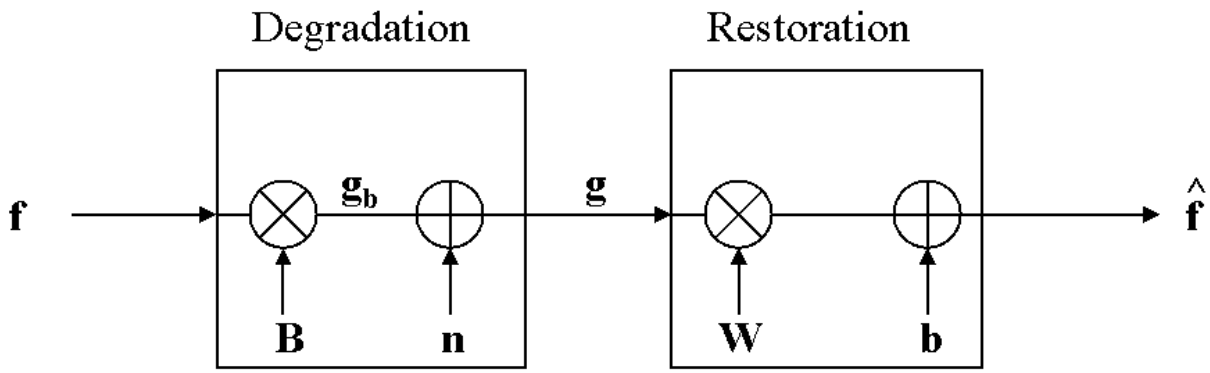

Figure 1. Wiener estimation for spatial image restoration. Explanations are given in the text.

Mathematically, this corruption is described in the vector-space model with

$$g = Bf + n \tag{1}$$

where g is the interferometric phase observation vector, f is the vector of the ideal interferogram and B is a matrix, whose elements are points on the impulse response function, often denoted as point spread function. The noise n is assumed to be zero mean with known covariance matrix K_n (Pratt, 1991).

For the restoration of g, an estimate $\hat{f}$ of the ideal image f is sought, which is given by

$$\hat{f} = Wg+b \tag{2}$$

where W is the restoration matrix and b is a bias vector. W and b are chosen for Wiener estimation in such a way that they minimize the mean-square restoration error e, which is defined as

$$e = E\{(f- \hat{f})^T(f- \hat{f})\} \tag{3}$$

Minimization of the least squares restoration error is achieved by applying the orthogonality principle, which yields two necessary and sufficient conditions for the determination of W and b.
Firstly, the expectation values of the estimate and the image must be equal:

$$E\{ f \} = E\{ \hat{f} \} \tag{4}$$

By substitution with (1) and (2), the bias b is given by

$$b = E\{ f \} - WE\{ g \} = E\{ f \} - WBE\{ f \} + WE\{ n \} \tag{5}$$

Secondly, the restoration error must be orthogonal to the observation centered at its mean:

$$E\{(f- \hat{f})(g - E\{ g \})^T\} = 0 \tag{6}$$

By further substitution and simplification, this yields (Pratt, 1991)

$$W = K_f B^T (BK_f B^T + K_n)^{-1} \tag{7}$$

where K_f and K_n are the image and noise covariance matrices.
Or, by expressing K_n and K_f by their energies $\sigma_n^2 I$ and $\sigma_f^2 I$,

$$W = B^T (BB^T + \sigma_n^2/\sigma_f^2)^{-1} \tag{8}$$

Certain aspects of the filter adaptation to the varying noise can directly be derived from (8).
In case that the image signal-to-noise ratio reaches infinity, i.e. no noise corrupt the fringes, the Wiener filter behaves equivalent to an inverse deconvolution filter with

$$W = B^{-1} \tag{9}$$

On the other hand, if the ratio approaches zero, W becomes 0 and therefore with (2) and (5)

$$\hat{f} = E\{ f \} \tag{10}$$

forcing a smooth solution in presence of extreme noise.
Finally, if the image signal is not blurred, i.e. B = I, W becomes

$$W = I(I + \sigma_n^2/\sigma_f^2)^{-1} \tag{11}$$

indicating the low-pass properties of the filtering in the special case of only additive phase noise.

Although Wiener filtering is theoretically the optimal method for the phase deconvolution in presence of noise, several problems limit its effectiveness.
Firstly, the precise knowledge of the ideal image f and the noise term n can not be assumed for most applications including this one. Models, developed for the direct approximation of B, are too weak for the highly complex phase restoration task. Secondly, the assumption of spatially invariant degradations for the whole image is not valid for the spatial variant interferometric signature. Thirdly, the image and noise signals are assumed to be stationary, which is hardly valid in mixed terrain.
In order to overcome limitations two and three, the proposed Wiener filtering will be applied locally, depending on the local SNR. The degradations behave spatially invariant within the borders of a limited window. In addition, the local power spectrum will hardly change within the window in comparison to the whole interferogram, thus fulfilling the stationarity requirement for the Wiener filtering.
The absence of an ideal image will be overcome in this approach with a synthetic interferogram, simulated from a stereo-optical DEM. It serves as reference in those areas, where the interferometric phase determination fails, especially in layover areas. Though far from being perfect measurements, the simulated data will deliver here reliable information, as the optical DEM generation is much less error affected in steep terrain, due to the fact that layover does not occur with optical measurements.

3 REALIZATION OF THE WIENER PHASE ESTIMATION

3.1 Filter Development

3.1.1 Bias estimation. The local offset between the interferometric phase measurement and the simulated phases is computed with (5) in a small estimation window, where both the correlation coefficients of the simulated and the interferometric phases are maximal. The bias estimation window is located as near as possible to the degraded region indicated by its low coherence, which would spoil the results, if it was used for bias estimation.
In case of slightly degraded measurements, the matrix W becomes close to I and therefore

$$b = E\{f\} - E\{g\} \tag{12}$$

For the local filtering approach pursued here, the resulting bias estimate can be assumed constant within the whole restoration window.

3.1.2 Restoration function. In order to avoid the high computational and implementational cost for the numeric realization of (7) in the spatial domain, the validation of the assumptions made above is for the time performed in the Fourier domain, which allows a much faster processing. As the filtering is restricted locally, the results will suffer only little from the limitations of the Fourier domain processing. Andrews (1977) refers on the generalization of the filter equations of the vector-space domain from section 2 to the here implemented filter in the Fourier domain, which has been realized as a parameterized Fourier Wiener filter, with the transfer function

$$W(k,l) = B^*(k,l)[|B(k,l)|^2 + \gamma P_n(k,l)/P_s(k,l)]^{-1} \tag{13}$$

With B(k,l) being the complex point spread function and $P_n(k,l)/P_s(k,l)$ the inverse of the signal to noise ratio and γ is a filter design constant, which allows additional control over the filter behavior. If γ is set to 1, the filter behaves like the traditional Wiener filter, else the parameter emphasizes ($\gamma > 1$) or de-emphasizes ($\gamma < 1$) the noise and signal statistics. Note that all terms of (13) are expressed in the Fourier domain, indicated with the k an l pixel coordinates.

3.2 Estimation of the filter parameters

3.2.1 Synthetic interferogram computation. As input data for the proposed method, two measurements are used, the SAR interferogram and a stereo-optical DEM. First, a SAR interferogram (Fig. 2) has to be computed with the procedure given in detail in Prati (1994).
The relation of the topographic phase component $\Delta\phi$ and the terrain elevation h in slant range is obtained, after compensation for the flat terrain contribution, by

$$\Delta\phi \approx Kh \tag{14}$$

where K is a scalar, depending on the sensor and orbit parameters (Prati, 1994).

Applying (14) to the optical DEM points after a slant range conversion derives the second, independent interferometric data source, the synthetic interferogram. The baseline and sensor information, necessary for height to phase and slant-range conversion, and is obtained from the SAR sensor specification and ephemeris data. The result of the simulation is an unwrapped phase image is wrapped in a range between -π and π through a modulo 2π operation (Fig. 4).

3.2.2 Signal-to-noise ratio. As the SNR decides about the filter behavior, the correct determination of the SNR is inevitable for the successful phase restoration. In the InSAR case, determination of the SNR becomes a straightforward task, as this information is directly retrievable from the interferometric processing by computing the local coherence ρ from the complex SAR images X1 and X2

$$\rho = \frac{E\{X1 \cdot X2^*\}}{\sqrt{E\{X1 \cdot X1\}E\{X2 \cdot X2\}}} \tag{15}$$

High coherence indicates those areas, where phase estimation for DEM generation is reasonable (Fig. 3). The SNR can be expressed as a function of the coherence with

$$SNR = \frac{\rho}{1-\rho} \tag{16}$$

Note that a coherence estimate is computed within an estimator window from the flattened interferogram (Small, 1994), therefore the estimated phase noise depends on the size of the estimator window (Prati, 1994). Still, the estimated coherence is a very good measure for the local SNR.

3.2.3 Point spread function. Referring to Fig. 1, B(k,l) relates the ideal image F(k,l) to the output of the blurring G_b(k,l) before the noise addition. Both the ideal image f and the blurring are determined from the given data for the computation of B(k,l).
Though the simulated phases may give a good approximation of the ideal phase course, measures have to be taken in order to avoid the introduction of optical DEM errors into the interferometric processing chain. A weighting of the simulated phases with respect to their expected error is performed using their cross-correlation coefficient, originating from the SPOT image matching (Fig. 5). High cross-correlation indicates the similarity between stereo images to be matched, and therefore is a measure of reliability of the detection of conjugate points. Erroneous matching still occurs even if the correlation is high, often causing spikes i.e. points with high height deviation compared to the surrounding mean. These spikes are interpreted as uncorrelated random noise in the DEM adding to the local height variance. Therefore, points showing extreme height variance are excluded from the phase simulation, by giving them zero weight. In order to increase the number of valid phase measurements, thus minimizing holes in the ideal interferogram through the weighting, also highly coherent interferometric phase values ($\rho > 0.6$) are used in the computation of F(k,l).

A blurred interferogram is approximated by phase subsampling in azimuth direction by factor 6 followed by phase averaging for noise reduction. Although the resulting image g_b has a lower resolution, the noise level is massively reduced, hence it serves for the estimation of the point spread function, which is finally computed in the Fourier domain by

$$B(k,l) = G_b(k,l)F^{-1}(k,l) \tag{17}$$

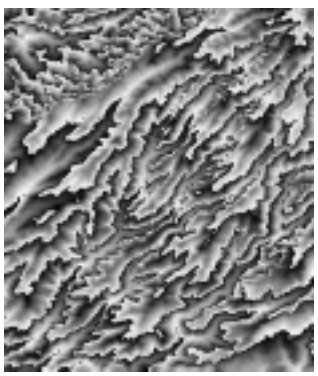
Figure 2. ERS-1, 3day-pass interferogram (~150km^2).

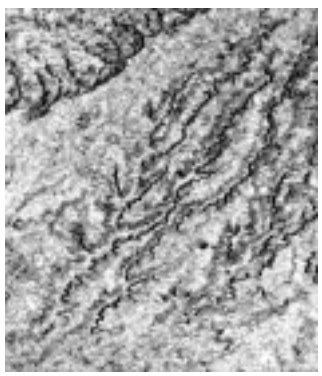
Figure 3. Phase coherence indicates the noise of Fig. 2.

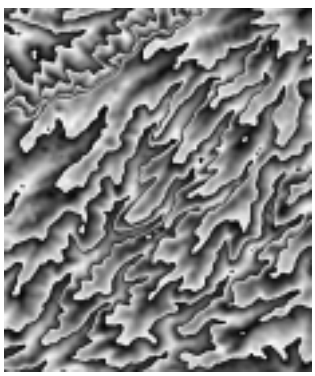
Figure 4. Interferogram, simulated a SPOT DEM.

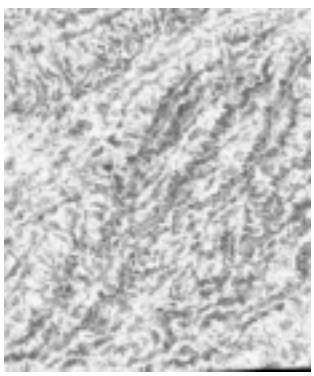
Figure 5. Cross-Correlation, from the point matching.

4 FUSION OF A SPOT STEREO DEM WITH AN ERS-1 INTERFEROGRAM

4.1 Test data

The test dataset consists of a pair of ERS-1 SLC quarter scenes (Frame 819, Quarter 1, Orbits 829 and 872), acquired in a three day interval (9/12/ and 9/15/91), and a SPOT stereo-pair, taken in a four day interval (9/3/ and 9/7/86). Both data sets are part of a data set of Catalonia used for our work in the EU project ORFEAS (Patias, 1998).
The test site comprises an area of approximately 150km^2 and shows an undulating terrain with a height difference of 315m between the minimal and maximal height. A DEM in 30m grid, derived from a 1:5000 topographic map, served as reference for our computations. The root mean square (rms) error of the reference DEM was approximately 1m.

The data has been processed with commercial software packages. The SPOT DEM is part of the DEM of the full scene, which has been generated by the Leica Helava DPW 770 digital photogrammetric workstation, which uses cross correlation for matching. The correlation coefficient of each point is not accessible directly, but is hidden behind a figure of merit (FOM). This FOM is in a range from 0 to 100 and is related to the correlation coefficient (Leica, 1997).
The SAR interferogram and the InSAR DEM have been generated with the PCI V6.1 IFSAR package. IFSAR offers also the opportunity for phase simulation from a given DEM. Both the original interferometric measurements and the results of the phase restoration are unwrapped with the ghost-line algorithm. Although the average coherence of the examined scene was relatively high ($\rho \approx 0.5$), due to the short repeat pass interval, several regions of low coherence have been observed and treated with the filter.
Due to lacking ground control points (gcp), 5 gcps have been derived from the reference DEM for geocoding and baseline estimation improvement. Baseline fitting has been performed by a technique, proposed by Werner (1992). The simulated phases have been registered in slant-range to the geometry of the interferogram with 12 manually collected tie-points.

4.2 Phase restoration

The Wiener filtering method has been applied to several regions within the interferogram, where the phase measurement initially failed. As the proposed method is spatially variant performing local filtering, certain regions of interest had to be found. As stated above, phase residuals, occurring due to noise or layover effects, are leading to phase unwrapping problems and were therefore targeted by the filtering. Residual reduction and the reconstruction of the fringe border are taken as measures of quality of the procedure. Residuals generally occur in presence of noise, hence coherence indicates the regions of interest to be treated with the Wiener filter. The coherence has therefore been used for the segmentation of the image in more and less affected regions. The filtering has been performed within a window of size 2^N x 2^M with natural numbers N and M required for the Fourier domain processing. Typical values for N and M, have been between 4 and 6.
The measurement problems occurring in the interferogram proved the error assumption of the degradation model of section 1. Two main error types have been encountered and consequently removed:

Fringe border degradation.
Occurring mostly due to aliasing effects, it endangers the whole height determination process, forcing manual treatment in form of fringe line editing. In part, the problems in these areas have been so severe that even manual editing of fringe line was not possible. Fig. 6 shows an example of degradations of this type, where residuals (positive residuals are given the color green, negative residuals are red) and the corrupted fringe border (yellow) are shown.
By applying the Wiener filter to these regions, the affected fringe borders could be restored completely. All occurring residuals vanished through the filtering, enabling smooth phase unwrapping even in those areas, in which the unwrapping originally failed. The fringe course could be estimated for those areas, where manual editing was initially not possible and had been excluded from the height determination process. As an example, the result of the filter operation, applied to Fig.6, is given in Fig. 7.

Local noise.
Noise occurs randomly within the fringes, due to decorrelation of the interferometric phases. These problems are less severe compared to the problems caused by the fringe border degradation, as they are locally restricted. Still, as they occur randomly, they require detection by their low coherence value followed by local treatment. Fig. 8 shows a typical example of random local noise.
The phase filtering performed also well with this type of degeneration. The affected areas have been smoothed according to the filter behavior in presence of additive noise. Adjacent valid fringe borders have not been affected from the filter operation proving the ability of the filter to adapt to the local noise (Fig. 9).

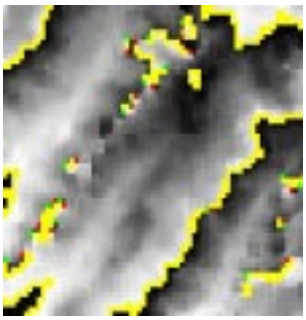
Figure 6. Degraded fringe borders.

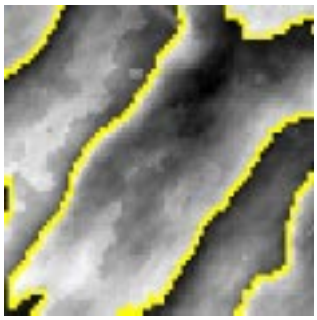
Figure 7. Restored borders after the Wiener filtering.

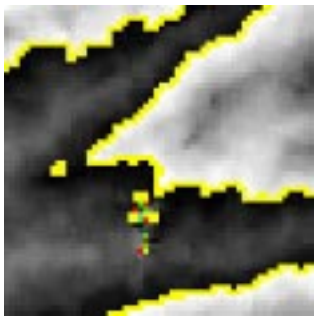
Figure 8. Random noise occurrence.


Figure 9. Noise removal by filtering.

4.3 Improvement of InSAR topographic height measurement

After the successful application of the filter to the phase noise reduction process, its impact on the interferometric height determination has been studied. A sub-region of the site of approximately 100km^2, containing 1.5 million phase measurements, has been selected from the ERS data sets for the DEM generation. The phase unwrapping has been performed with the ghost-line method. For the evaluation of the filtering, two DEMs, one with and the other without Wiener noise reduction (Fig. 10), have been produced and compared to the SPOT results and the reference DEM.
The SPOT and ERS DEMs have been sampled in a 30m grid and were compared to ground truth by bilinear interpolation of each height value in the reference DEM. The resulting error statistics in terms of mean, rms and the maximum errors are given in Tab. 1.

Error [m]	Stereo-Optical	InSAR	Wiener filtered InSAR
Mean	1.4	-2.9	2.1
RMS	8.4	20.8	5.5
$\sigma_{ex\text{-}min}$	-71.6	-139.4	-37.6
$\sigma_{ex\text{-}max}$	104.4	84.6	33.1

Table 1. Error statistics of the SPOT, ERS-1 and filtered SAR-optical DEM

In comparison to the original interferometric height measurements, the Wiener enhanced InSAR DEM shows improved statistics in all categories. The relatively high mean error may be a result of the gcp determination. The difference of 5m for the mean between the InSAR DEMs indicates the systematic changes due to the Wiener filtering. The Wiener InSAR DEM is considerably improved with respect to the rms error, which decreased by 74%, and maximum errors, both being fractions of the original ones.
InSAR and stereo-optical height measurements achieve an initial rms error, which is beneath the pixel resolution of the sensor (SPOT: 10m, ERS-1: 23m). The initial pixel resolution is a fact that is hardly considered, when comparing the InSAR with stereo-optical DEMs. In this context, it is most remarkable that the Wiener InSAR DEM is superior to the SPOT height measurements in rms (-35%) and maximum errors, again considerably reduced. No errors higher than 37.6m occurred in the improved InSAR DEM, while in the original InSAR DEM 27.2% and in the SPOT DEM 2.4% of all values showed an error higher than 40m. None of the extreme corrupted measurements of the SPOT DEM entered the fusion process due to the weighting procedure.
These results emphasize the interferometric height measurement capabilities in case of restored phases. It is important to note that the InSAR measurements have been improved with the simulated phases to an extent that the quality of the result is higher than the assumed ideal data source.
Finally, the amount of measurements has been increased by this method from 113.000 points, originating from the SPOT measurements, to more than 118.000 points in the improved InSAR DEM.

5 CONCLUSIONS

A new method for the fusion of optical and SAR interferometric data by applying Wiener filtering for phase restoration has been introduced and tested. It reduces the effect of noise on the interferometric height determination, namely the degradation of fringe borders, typically caused by layover, and the occurrence of local phase noise, e.g. due to vegetation. In this way, new interferometric height measurements, like from SRTM, can be related to and enhanced with former photogrammetric measurements. The presented procedure helps overcoming the limitations of the interferometric height determination, by taking advantage from the synergy between optical and SAR height measurements in critical areas. The noise-adaptive data fusion process preserves valid interferometric measurements,

while restoring them in case of degradation. In order to avoid the introduction of corrupted measurements in the fusion process, an attribute has been derived, indicating the expected error of the measurement.
This local approach leads to a global improvement of the resulting height measurements with respect to

- Amount of valid measurements (reduction of measurement holes)
- DEM error distribution
  - Reduction of mean and root mean square error
  - Extreme reduction of outliers.

The achieved results are much superior compared to the initial results from the single sensor data sources and encourage the work on a complete numerical realization of the Wiener phase estimation in the spatial domain.

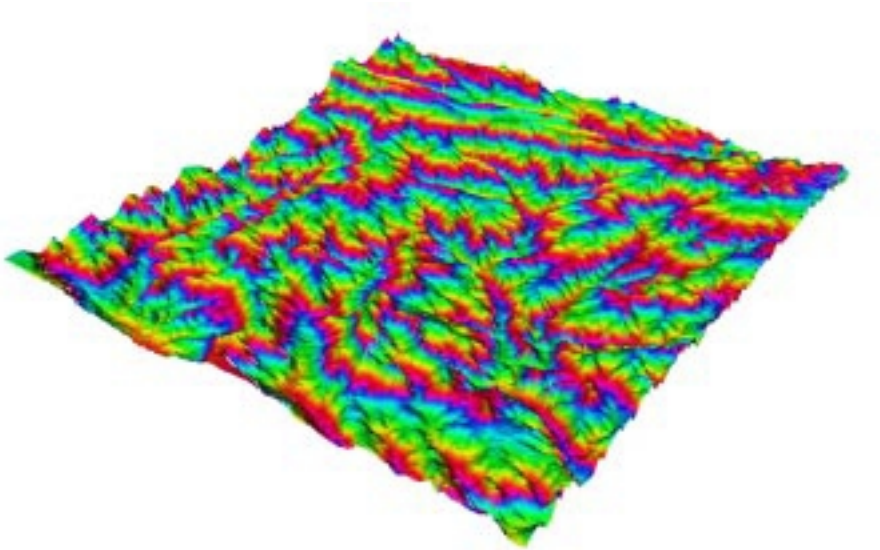

Figure 10. Restored interferogram draped over the Wiener improved elevation model

REFERENCES

Andrews, H., Hunt, B., 1977. Digital Image Restoration, Prentice Hall Int., New Jersey, pp. 147-151.

Goldstein R., Zebker H., Werner C., 1988. Satellite Radar Interferometry: Two dimensional phase unwrapping. Radio Sci., vol. 23, no.4, pp. 713-720.

Honikel, M., 1998. Fusion of Optical and Radar Digital Elevation Models in the Spatial Frequency Domain, Proc. 2nd Int. Workshop Retrieval of Bio- and Geophysical Parameters from SAR Data, ESTEC, Nordwijk, pp. 537-543.

Honikel, M., 1999. Data Fusion Strategies for the Fusion of InSAR and Stereo-Optical DEMs, Int. Archives of Photogrammetry and Remote Sensing, Vol. 32, Part 7-4-3 W6, pp. 83-89.

Leica Helava, 1997. SOCET SET, Windows NT/UNIX User Manual, Release 4.0, pp. F-1-4.

Pratt, W. K., 1991. Digital Image Processing, 2nd ed., John Wiley & Sons New York, pp.384-385.

Patias, P. (ed.), 1998. ORFEAS, Optical Radar Sensor Fusion for Environmental Applications, Final EU Project Report, Contract no. ENV4-CT95-0150.

Prati, C., Rocca, F., Monti-Guarnieri, A., Pasquali, P., 1994. ERS-1 Interferometric Techniques and Applications, ISPRS Proceedings of Primary Data Acquisition and Evaluation, 30(1), pp. 123-126.

Small D., Werner, C., Nüesch, D., 1994. Geocoding and Validation of ERS-1 InSAR-Derived Digital Elevation Models, EARSel Advances in Remote Sensing, 4(2)-X, pp.26-41.

Werner, C., 1992. Techniques and Applications of SAR Interferometry for ERS-1: Topographic Mapping, Change Detection and Slope Measurement. Proc. 1st ERS-1 Symposium, Space at the Service of our Environment, pp.205-210.

Zebker, H., Werner, C., Rosen, P., 1994. Accuracy of Topographic Maps Derived from ERS-1 Interferometric Radar, IEEE Transactions on Geoscience and Remote Sensing, 32(4), pp. 823-836.